Appl Biochem Biotechnol
DOI 10.1007/s12010-015-1643-x

# Ultrasensitive Impedimetric Biosensor Fabricated by a New Immobilisation Technique for Parathyroid Hormone

**Hakkı Mevlüt Özcan**[1] · **Kübra Yildiz**[1] · **Cansu Çakar**[1] · **Tuba Aydin**[1] · **Engin Asav**[2] · **Ayten Sağiroğlu**[1] · **Mustafa Kemal Sezgintürk**[3]

Received: 5 February 2015 / Accepted: 21 April 2015


**Abstract** This paper presents a novel ultrasensitive and rapid impedimetric biosensor with new immobilisation materials for parathyroid hormone (PTH) with the aim to determine the PTH level in serum for the diagnosis and monitoring of parathyroid diseases such as hyperparathyroidism, adenoma, and thyroid cancer. The interaction between PTH and the biosensor was investigated with an electrochemical method. The biosensor was based on the gold electrode modified by mercaptohexanol (6-MHL). Anti-parathyroid hormone (anti-PTH) was covalently immobilised onto a self-assembled monolayer (SAM) by using epiclorhidrina (EPI) with ethanolamine (EA). The EPI-EA interaction represents the first use of these for the construction of biosensors in published reports. The immobilisation of the anti-PTH was monitored by electrochemical impedance spectroscopy, cyclic voltammetry and scanning electron microscopy (SEM) techniques. After the optimisation studies of immobilisation materials such as 6-MHL, EPI, EA and glutaraldehyde, linearity, repeatability and sensitivity of biosensor were evaluated as the performance of biosensor. PTH was detected within a linear range of 0.1–0.6 pg/ml, and the detection limit was 0.1 fg/ml. The specificity of the biosensor was also investigated. Finally, the described biosensor was used to detect the PTH levels in artificial serum samples.

**Keywords** Parathyroid hormone · Biosensor · Epiclorhidrina · Electrochemical impedance spectroscopy · 6-mercaptohexanol

**Electronic supplementary material** The online version of this article (doi:10.1007/s12010-015-1643-x) contains supplementary material, which is available to authorized users.

✉ Hakkı Mevlüt Özcan
ozcanhakki@gmail.com

[1] Chemistry Department, Faculty of Science, Trakya University, Edirne, Turkey

[2] School of Health, Kırklareli University, Kırklareli, Turkey

[3] Chemistry Department, Faculty of Arts and Sciences, Namık Kemal University, Tekirdağ, Turkey

Published online: 03 May 2015

## Introduction

Parathyroid hormone or parathormone (PTH) is secreted by the chief cells of the parathyroid glands as a polypeptide containing 84 amino acids. It is used worldwide to treat millions of patients with parathyroid disorders. In primary hyperparathyroidism, 80–85 % is due to PTH hyper secretion from a solitary parathyroid adenoma, which may present with nephrolithiasis, hypercalcemia, depression, osteopenia, peptic ulcer disease, pancreatitis and proximal muscle weakness. Other causes of primary hyperparathyroidism include parathyroid gland hyperplasia (10 %), multiple parathyroid adenomas (4 %) and parathyroid carcinoma (1 %) [1–5]. The half-life of the PTH is very short at 3 to 5 min, and excision of the parathyroid tissue is followed by a rapid fall in serum normal levels of 11–54 pg/ml. PTH assays, with a turnaround time of 15–20 min, have made intraoperative PTH analysis a reality in various centres [6–8]. Therefore, sensitive and rapid PTH detection in serum samples is vital for diagnosis and monitoring of treatment.

Electrochemical impedance spectroscopy (EIS) is a very powerful tool with ultra-high sensitivity. EIS is effective for the analysis of changes in interfacial properties of modified electrodes upon biorecognition events occurring at the modified electrode surfaces. This technique provides detailed information on capacitance and resistance changes occurring at electrode surfaces [9]. Therefore, there is a wide range of EIS-based biosensors that are utilised for monitoring the relation between specific molecules such as proteins, nucleic acids, receptors, whole cells, antibodies and enzyme reactions [10–13].

The modification of electrode surfaces is extremely important in assay and EIS-based biosensor development because it ensures the selective capture and detection of the targets of interest. Disulfides, sulphides or thiols coordinate very strongly onto a variety of metals, e.g. gold, silver, platinum or copper. The structure of a self-assembled monolayer (SAM) depends on the morphology of the metal. Gold is the metal most commonly used in the formation of SAMs. Gold films predominantly adopt the ideal crystallographic orientation and it is favoured because it is reasonably inert [14, 15]. Ideally, the SAM has to be composed of tightly packed and well-ordered chains, although several factors may lead to the formation of defects and irregularities [16]. Some scholars have reported their successful use of SAM-based impedimetric biosensors [17–20].

Alkanethiols on a gold surface provide a class of well-controlled organic monolayers. Some research groups have used mercaptohexanol (6-MHL) as an alkanethiol for the aim of forming a SAM on gold surfaces [14, 21]. Baldrich et al. have activated 6-MHL with epiclorhidrina (EPI) and conjugated with CM-Dextran for protein and bacteria detection. In this study, ethanolamine (EA) was used as a linker between the SAM activated by EPI on the gold electrode surface and the receptor, the first time this has been done in a published report. EA, also called 2-aminoethanol or monoethanolamine, is an organic chemical compound that is both a primary amine and a primary alcohol. The hydroxyl group of EA gives a substitution reaction with the chloride groups of EPI and forms a Schiff base with glutaraldehyde (GLT), which is a cross linker between the receptor and electrode surface.

The objective of this study is to develop an electrochemical biosensor system based on EIS that will enable rapid, ultra-sensitive and practical determination of the PTH for the monitoring of parathyroid diseases. A SAM strategy with new immobilisation materials for introducing an immobilisation platform on the gold electrodes is reported in this study. To form SAM, 6-MHL was used. Anti-parathyroid hormone (anti-PTH) is covalently attached to the SAM of EPI with the help of GLT and EA, which is the first time this has been done in any of the published

literature. The proposed biosensor can detect concentrations of the PTH in very low levels. This study also identified scanning electron microscopy (SEM) features of the surfaces of each layer based on a combination of EIS in the presence of $[Fe(CN)_6]^{3-/4-}$ as a redox couple. Finally, artificial serum samples spiked with PTH were analysed by the biosensor.

## Experimental

### Materials and Instrumentation

All reagents were of analytical grade, unless otherwise stated, and were purchased from Sigma-Aldrich (St. Louis, Missouri, USA). PTH and anti-PTH were purchased from Sigma-Aldrich (St. Louis, Missouri, USA). PTH and anti-PTH portions were prepared at certain concentrations and were stored at −20 °C until use. Artificial serum solution was prepared by using 4.5 mM KCl, 5 mM $CaCl_2$, 1.6 mM $MgCl_2$, 4.7 mM D(+) glucose, 2.5 mM urea, 0.1 % human serum albumin and 145 mM NaCl. A three-electrode system, consisting of a gold working electrode (with a surface area of 2.01 $mm^2$), Ag/AgCl (saturated KCl) reference electrode and a Pt counter-electrode, was accommodated in a 5-ml electrochemical cell (all electrodes were obtained from iBAS, Warwickshire, UK). Electrochemical experiments were performed using a Gamry Interface 1000 Potentiostat/Galvanostat (Gamry Instruments, Warminster, Pennsylvania, USA) interfaced with a PC via an EChem Analyst containing physical electrochemistry, pulse voltammetry and EIS software (Gamry Instruments, Warminster, Pennsylvania, USA). In all of the electrochemical experiments, a Faraday cage (from iBAS, Warwickshire, UK) was used to block out external static electric fields.

### Modification of the Gold Electrodes by 6-MHL

Before use, the gold electrodes were first polished with 0.05-μm alumina powder and then washed with ultrapure water. Following that, the electrodes were ultrasonically washed in absolute ethanol for 3 min to remove any alumina residue. Then, the surfaces of the electrodes were dried by an ultra-pure argon stream. This polishing and cleaning procedure was repeated before every electrode preparation step. The clean gold electrodes were immediately immersed into 5 mM 6-MHL solution for 16 h. After this period, they were rinsed with ethanol and gently dried with an ultra-pure argon stream.

### Covalent Attachment of Anti-PTH on 6-MHL-modified Gold Electrodes

For anti-PTH immobilisation, EPI, EA and GLT were used. The chloride groups of EPI give a substitution reaction with the hydroxyl groups of EA and form ether. After this reaction, the amino groups of EA react with the aldehyde group of GLT, and a Schiff base is formed. The other aldehyde group of GLT reacts with the amino groups of anti-PTH amino acids. For the purposes of this study, an EPI solution (20 %) was spread over the electrode surface and then left for 45 min in a dark medium. For the next step, EA (0.5 M) was dropped on the electrode surface and was left for 60 min. Then, a GLT solution (1.5 %) was dropped on the electrode surface and left for 15 min. At the end of each step, the electrodes were gently washed with ultra-pure water and then dried by an ultra-pure argon stream again. A 5-μL portion of anti-PTH was spread over on the active electrode surface, and the electrode was incubated for an

hour in a humid medium. Finally, the electrode was washed with ultra-pure water to remove physically adsorbed anti-PTH molecules. Bare gold electrodes and the modified electrodes were denoted as Au, Au/6-MHL, Au/6-MHL/EPI, Au/6-MHL/EPI/EA, Au/6-MHL/EPI/EA/GLT, Au/6-MHL/EPI/EA/GLT/anti-PTH and Au/6-MHL/EPI/EA/GLT/anti-PTH. All of these steps are summarised in Fig. 1.

### Electrochemical Studies

Electrochemical impedance and cyclic voltammetry measurements were carried out in 5 mM of $K_3[Fe(CN)_6/K_4[Fe(CN)_6]$ (1:1) solution, which served as a redox probe containing 0.1 M KCl. In the cyclic voltammetry studies, the potential was varied between −0.5 and 1 V (step size, 20 mV; scan rate, 50 mV/s). For electrochemical impedance measurements, an alternating wave with an amplitude of 10 mV was applied to the electrode. In the potentiostatic mode, the electrochemical impedance experiments were done at a fixed DC potential of 0 V. The redox couple used for impedance studies was the same as that used for the cyclic voltammetry. Impedance spectra were collected in the frequency range between 10,000 and 0.05 Hz.

### Scanning Electron Microscopy Investigations

Structural observations of a surface modified by immobilisation and PTH binding were performed by a field-emission scanning electron microscope (SEM) (EVO/LS10 ZEISS) at the Technology Research and Development Centre of Trakya University. An acceleration voltage of 5 kV was used to acquire SEM images.

## Results and Discussion

### Anti-PTH Immobilisation

The cyclic voltammograms and EIS spectra of each immobilisation step of the anti-PTH are shown in Figs. 2 and 3. Each immobilisation step is well defined by a redox couple. When the electrode was covered by the 6-MHL SAM, the peak current was increased because the hydroxyl groups of 6-MHL probably prevented from reaching the negatively charged ferricyanide to the electrode surface. As shown in Fig. 2, the characteristic cyclic voltammetry (CV) peaks of the electrode could be seen after the 6-MHL modification of the electrode surface. After the EPI reacted with the 6-MHL, the charge-transfer resistance ($R_{ct}$) was seen to be less than 3 kΩ. Since the hydroxyl groups of 6-MHL were activated by negatively charged EPI, the

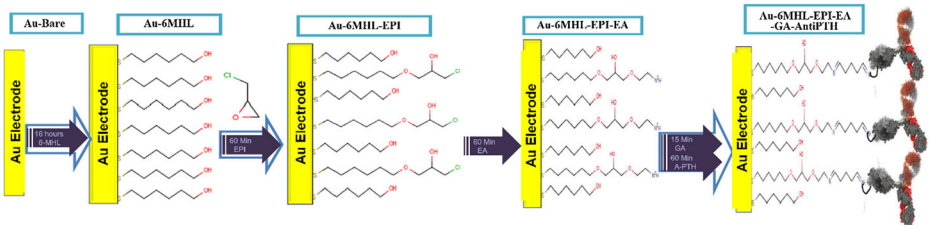


**Fig. 1** Schematic representation of the fabrication of biosensor

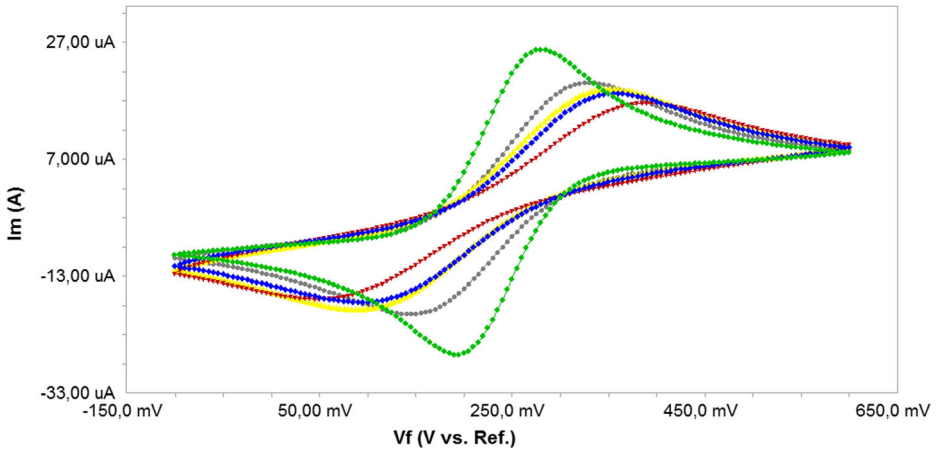


**Fig. 2** Electrochemical characterisation of PAMAM-based anti-PTH biosensor [cyclic voltammograms related with anti-PTH immobilization by covalently attachment [-■-■-(*green*): bare gold electrode, -●-●- (*grey*):6MHL, -♦-♦-(*blue*):6MHL-EPI, -▲-▲- (*yellow*): 6MHL-EPI-EA, -▼-▼-(*red*): 6MHL-EPI-EA-Anti-PTH]

negatively charged redox probes were absorbed by the surface of the electrode. Therefore, characteristic CV peaks of the conductor surface could be seen. Amino groups of EA are positively charged at a pH of 7. After the EA modification of the surface, the further positively charged groups were absorbed by the negatively charged ferricyanide to the electrode surface. Consequently, the $R_{ct}$ was decreased. Similarly, when the $R_{ct}$ was decreased, the CV peak was increased because of the high current. Covalent immobilisation of anti-PTH on the surface enhanced the insulating property of the electrode surface, and this resulted in an increase of the $R_{ct}$ and a decrease of the CV peak, which could be seen in cyclic voltammograms and EIS spectra.

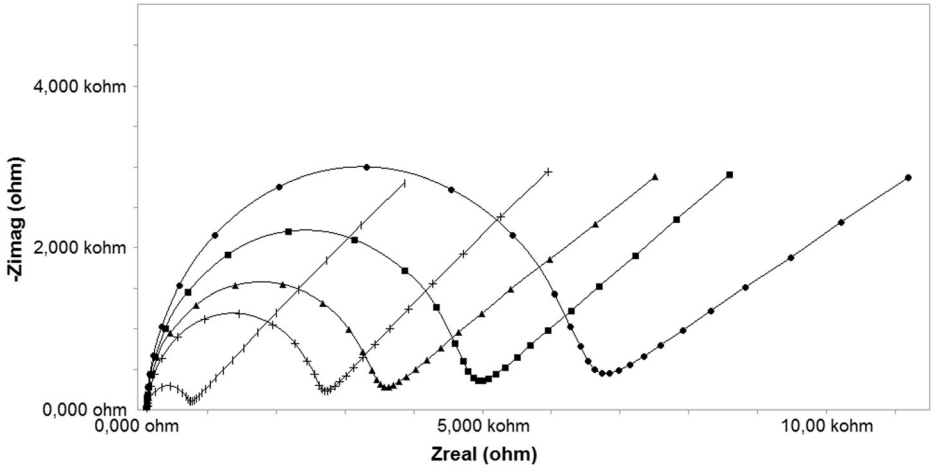


**Fig. 3** Electrochemical impedance spectra of anti-PTH immobilization steps [*inset figure*: -|-|-: bare gold electrode, -+—+-: 6MHL, -■-■–: 6MHL-EPI, ▲-▲-: 6MHL-EPI-EA, -●-●-: 6MHL-EPI-EA-Anti-PTH]

## Scanning Electron Microscopy Investigations

To monitor the construction of the biosensor and the binding of the PTH, SEM was used. The SEM images are shown in Fig. 4a–e. which show, respectively: Au the bare electrode; after 6-MHL modification (Au-6-MHL); after EPI modification (Au-6-MHL-EPI); after anti-PTH immobilisation (Au-6-MHL-EPI-EA-GLT-anti-PTH) and after PTH binding (Au-6-MHL-EPI-EA-GLT-anti-PTH-PTH). Obviously, as can be seen in these images, the immobilisation steps and the binding of PTH to the biosensor were successful.

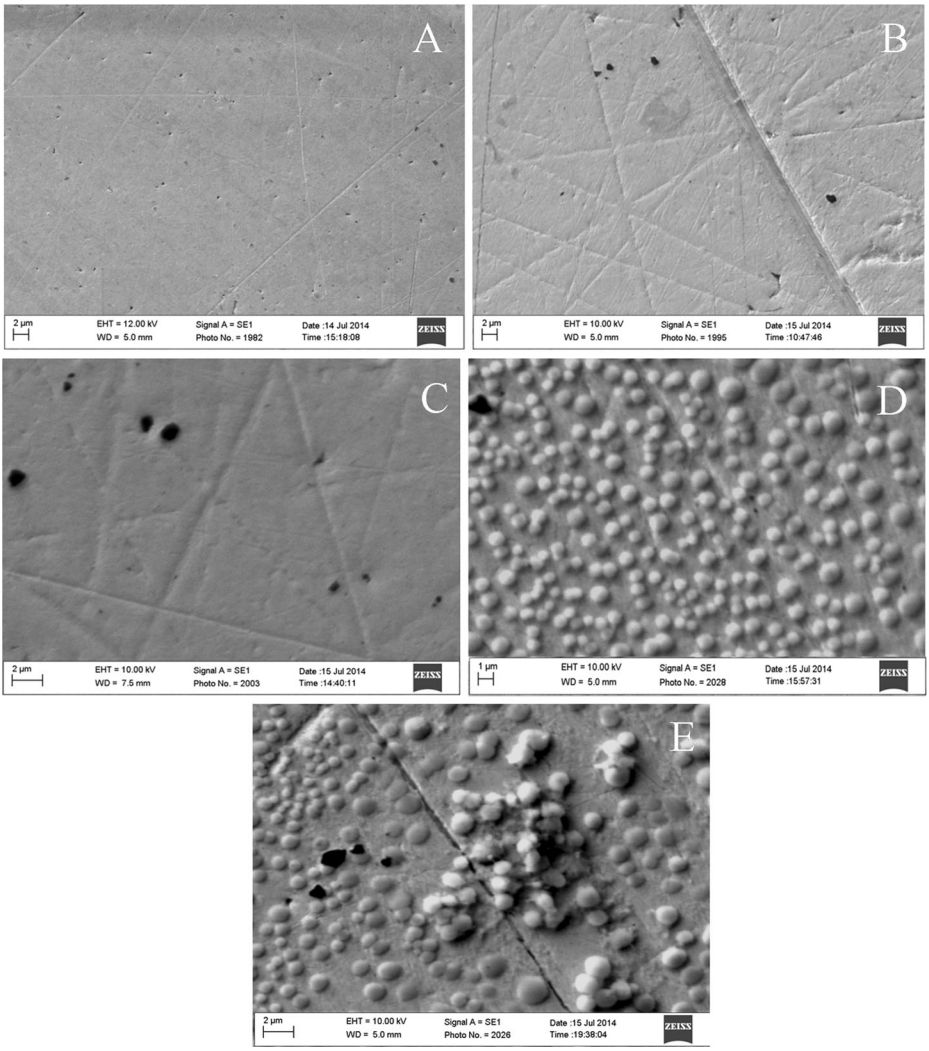


**Fig. 4** SEM investigations of the biosensor surfaces. [SEM images: **a** bare gold electrode, **b** Au-6MHL, **c** Au-6MHL-EPI-EA-GLT, **d** Au-6MHL-EPI-EA-GLT-Anti-PTH and **e** Au-6MHL-EPI-EA-GLT-Anti-PTH-PTH]

## Optimisation of the Biosensor

Layer-by-layer preparation of the biosensor was investigated in terms of its effect on 6-MHL concentration, EPI concentration, EA concentration, GLT concentration and anti-PTH concentration.

In order to explain how 6-MHL concentration effect to the biosensor response, 1–6 ng/ml of PTH standard solutions were separately analysed by biosensors prepared with different concentration of 6-MHL (2, 5, 10 and 20 mM). As seen in Fig. 1s, $R^2$ values were calculated as 0.9467, 0.9282, 0.8927 and 0.8693, respectively. In addition, 4 pg/ml of PTH standard solutions were separately analysed by different biosensors to investigate the effect of 6-MHL concentrations on $R_{ct}$. The spectra of the experiments are shown in Fig. 2s. The $R_{ct}$ values were 1.79, 4.92, 1.15 and 2.32 kΩ, respectively. Because the best linearity and the highest $R_{ct}$ value were found at 5 mM of 6-MHL concentration, that particular concentration was deemed ideal and used in all of the experiments after this step.

The next step in the optimisation studies related to the concentration of EPI. For this investigation, 1, 5, 10 and 20 % EPI concentrations were used for the construction of the biosensors. PTH standard solutions of 1–6 ng/ml were separately analysed by biosensors to investigate the linearity of biosensor responses; additionally, 4 ng/ml PTH standard solutions were separately analysed by different biosensors to compare $R_{ct}$ values. As seen in Fig. 3s, $R^2$ values were calculated as 0.9680, 0.9401, 0.9287 and 0.9948, respectively. The impedance spectra are shown in Fig. 4s. $R_{ct}$ values were 4.61, 6.82, 4.50 and 4.42 kΩ, respectively. The rise of the EPI concentration led to a smoother surface, thereby increasing the linearity of the biosensor responses. Although a maximum $R_{ct}$ value could not be obtained with a 20 % EPI concentration, the 20 % EPI concentration was chosen as the optimal concentration. The EPI incubation period was also investigated. For this, 1 – 6 ng/ml of PTH standard solutions were separately analysed by biosensors prepared using 20 % EPI solution at 30, 45, 60 and 75-min incubation periods. The results of these experiments are shown in Fig. 5s. $R^2$ values were calculated as 0.9720, 0.9944, 0.9941 and 0.9675, respectively. When the incubation period was increased (75 min), the amount of evaporated solvent of EPI increased. Therefore, the EPI concentration of the electrode surface decreased. Because of the lower EPI concentration on the electrode surface, the response of the biosensor decreased. At 45 and 60-min incubation periods, almost equal $R^2$ values were obtained. Because of the time advantage, 45 min was chosen as the optimal incubation period of EPI.

The biosensors were prepared by using 0.1, 0.5 and 1 M of EA solutions for the optimisation of the EA concentration study. For this investigation, the experiments were done under the same conditions described above. The results can be seen in Fig. 6s. $R^2$ values were calculated as 0.9928, 0.9601 and 0.9575, respectively. $R_{ct}$ values were 1.77, 3.64 and 2.37 kΩ, respectively, and these are shown in Fig. 7s. It was expected that when the EA concentration was increased, the amount of bound anti-PTH on the electrode surface would also increase. But the higher EA concentration could lead to EA molecules being closer on the surface, resulting in the formation of amine bridges between each molecule. Therefore, the amount of bound anti-PTH on the electrode surface decreased while the $R_{ct}$ value also decreased. Because of the linear response profile of the biosensor, the 0.5 M of EA concentration was chosen as the optimal value. For the EA incubation study, the experiments were done by biosensors that

were prepared using 0.5 M of EA solution at 30-, 60- and 75-min incubation periods. The results are shown in Fig. 8s. $R^2$ values were calculated as 0.9622, 0.9980 and 0.9635, respectively. According to the response linearity, 60 min was chosen as the optimal incubation period for EA immobilisation.

Next, the biosensors were prepared with different GLT concentrations (0.5, 1.25 and 2.5 %) to determine the optimal GLT concentration. The experiments were carried out under the same conditions described above. The $R^2$ and $R_{ct}$ values are shown in Fig. 9s and Fig. 10s, respectively. $R^2$ values were calculated as 0.9535, 0.9960 and 0.9190, respectively, while $R_{ct}$ values were 1.95, 2.05 and 1.08 kΩ, respectively. The higher GLT concentration (2.5 %) leads to a decrease in biosensor response because if the amount of cross linker on the electrode surface is increased, then the amount of unwanted bonds between anti-PTH molecules also increases. According to the response linearity, the 1.25 % GLT solution was chosen as the optimal GLT concentration.

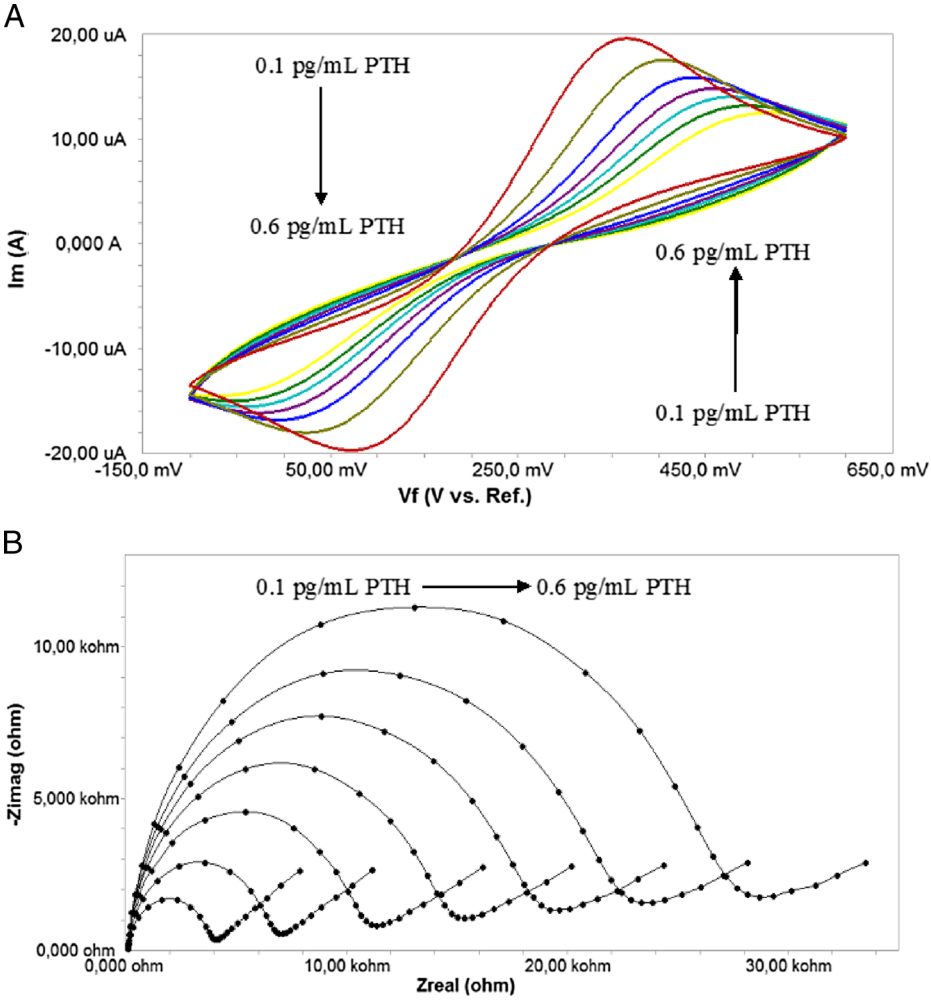


**Fig. 5** **a** Cyclic voltammograms of the biosensor for different PTH concentrations. **b** Nyquist plots of the biosensor for different PTH concentrations

In the last step of the optimisation studies, the effect of the anti-PTH concentration on the biosensor response was investigated. For this, 1–6 ng/ml of PTH standard solutions were separately analysed by biosensors prepared with different concentrations of anti-PTH (5, 10 and 15 ng/5 μL). As seen in Fig. 11s, $R^2$ values were calculated as 0.9030, 0.9892 and 0.9981, respectively. Higher concentrations of anti-PTH (15 ng/5 μL) resulted in denser bonds between PTH and anti-PTH. Therefore, the higher anti-PTH concentrations lead to higher $R_{ct}$ values. This situation was expected. According to the response linearity and $R_{ct}$ values, the 15 ng/5 μL anti-PTH concentration was chosen as the optimal concentration.

## Analytical Procedure and Sample Analyses

The described biosensor was characterised on account of linear range, reproducibility and repeatability. In this study, EIS was successfully used to determine the amount of PTH on the electrode surface associated with changes in the charge transfer resistance of the biosensor. To obtain linear relation between PTH concentrations and electrochemical signals, the absolute impedance values were used. A simple equation: $\Delta R_{ct} = R_{ct(PTH)} - R_{ct(anti\text{-}PTH)}$ was used to calculate the impedance changes, $R_{ct(PTH)}$ and $R_{ct(anti\text{-}PTH)}$ are the electron transfer resistances of the electrode surface before and after anti-PTH is coupled with PTH, respectively. As can be seen from Fig. 5a, cyclic voltograms (CV) showed that peak currents decreased with an increase in the PTH concentrations.

Nyquist plots of the developed biosensor for different PTH concentrations are shown in Fig. 5b. It is clear from the figure that increasing PTH concentration is led to increase the semi-circle diameter in the Nyquist plots. Moreover, concentration-dependent analysis can be performed in low frequencies. The incremental increase of PTH concentration increased the charge transfer resistance. The detection range of 0.1–0.6 pg/ml was chosen because

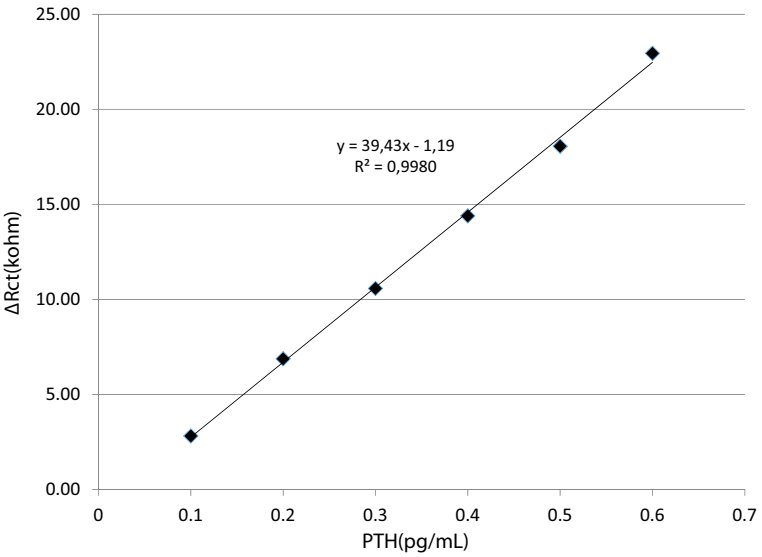


**Fig. 6** PTH calibration curve

the normal level of PTH in serum is 11–54 pg/ml [7]. The results revealed that the described biosensor allowed the determination of PTH in an extremely sensitive manner. Figure 6 shows the calibration graph of biosensor that was drawn according to the variations in $R_{ct}$ after PTH applications. Dittmer et al. have described giant magnetoresistive biosensors for PTH determination [22]. They used 300 and 500 nm of actuated magnetic particles for construction of biosensors, and they have reported 95 and 7.6 pg/ml detection limits, respectively. A commercial immunoassay test kit based on enzyme immunoassay is available for laboratories. This product can detect PTH in serum samples with 1.27 pg/ml of detection limit. Moreover, Özcan and co-workers recently reported a biosensing system based on Cysteine SAM coupled with well-known EDC/NHS chemistry [23]. In this system, the linear calibration range for PTH was 10–60 fg/mL; however in our system, EPI activation of –COOH ends was the most important novelty. Besides, in the presented study, the recovery and relative differences values obtained in the artificial serum sample analyses were better than the previous reported study.

The present biosensor was investigated in terms of the reproducibility. For the purpose of this study, nine different biosensors were constructed by the same procedures and tested at same detection range. The results indicated that the biosensor can be reproducibly used for PTH detection and quantification. The results can be seen in Table 1.

Additionally, the artificial serum samples spiked with PTH were analysed by the biosensor. Results of six different measurements can also be seen in Table 1. These results show that the PTH levels in the artificial serum samples analysed by described biosensor agreed with the spiked amount of the artificial serum samples.

**Table 1** The reproducibility of the biosensor and the results for serum sample analysis

| Biosensor numbers | $R^2$ | $y$ | Linear ranges (pg/mL) |
|---|---|---|---|
| 1 | 0.999 | $y=24.32x-0.08$ | 0.1–0.6 |
| 2 | 0.995 | $y=29.477x-0.358$ | 0.1–0.6 |
| 3 | 0.995 | $y=39.72x-0.105$ | 0.1–0.6 |
| 4 | 0.992 | $y=38.505x+0.225$ | 0.1–0.6 |
| 5 | 0.989 | $y=44.74x-1.623$ | 0.1–0.6 |
| 6 | 0.992 | $y=37.62x-2.571$ | 0.1–0.6 |
| **7** | 0.997 | $y=37.64x-1.153$ | 0.1–0.6 |
| 8 | 0.995 | $y=34.80x-0.329$ | 0.1–0.6 |
| 9 | 0.999 | $y=35.57x-0.408$ | 0.1–0.6 |
| PTH detections in artificial serum samples | | | |
| Added PTH (pg/mL) | Found by biosensor (pg/mL) | Recovery (%) | Relative differences (%) |
| 0.1 | 0.1011 | 101.1 | 1.60 |
| 0.2 | 0.2012 | 100.6 | 0.60 |
| 0.3 | 0.3008 | 100.2 | 0.20 |
| 0.4 | 0.3984 | 99.60 | 0.40 |
| 0.5 | 0.4982 | 99.64 | 0.36 |
| 0.6 | 0.6001 | 100.01 | 0.01 |

## Conclusion

This study describes the development of a simple electrochemical biosensor for the detection of PTH with ultrahigh sensitivity and which could be an effective method to analyse the interactions between PTH and anti-PTH. The immobilisation of the anti-PTH on 6-MHL with EPI-EA-modified gold electrodes was simple, effective and a first in published reports. The biosensor was characterised in depth using CV and EIS. The proposed biosensor is highly reproducible and is able to detect PTH in a linear range of 0.1–0.6 pg/ml.

**Acknowledgments** Support from the Trakya University Scientific Research Foundation (project number: TUBAP-2001/195) and TÜBİTAK (The Scientific and Technological Research Council of Turkey; project number: 113 Z 678) are greatly acknowledged.

## References

1. Eleraj, D. M., & Clark, O. H. (2008). Current status and treatment of primary hyperparathyroidism. *The Permanente Journal, 12*, 32–37.
2. Lendel, I., & Horwith, M. (2004). An update from the latest workshop on asymp-tomatic primary hyper-parathyroidism. *Otolaryngologic Clinics of North America, 37*, 737–749.
3. Kukora, J. S., Zeiger, M. A., & Clark, O. H. (2005). The American association of clinical endocrinologists and the American association of endocrine surgeons position statement on the diagnosis and management of primary hyperparathyroidism. *Endocrine Practice, 11*, 49–54.
4. Suliburk, J. W., & Perrier, N. D. (2007). Primary hyperparathyroidism. *The Oncologist, 12*, 644–653.
5. Sosa, J. A., & Udelsman, R. (2008). The parathyroid glands. In R. Beauchamp, B. Evers, & K. Mattox (Eds.), *Sabiston textbook of surgery* (18th ed., pp. 955–975). Philadelphia: P.A Saunders.
6. Ohe, M. N., Santos, R. O., Kunii, I. S., Abrahão, M., Cervantes, O., Carvalho, A. B., Castro, M. L., & Vieira, J. G. H. (2006). Usefulness of intraoperative PTH measurement in primary and secondary hyperparathy-roidism: experience with 109 patient. *Arquivos Brasileiros de Endocrinologia e Metabologia, 50*, 869–875.
7. Aloia, J. F., Feuerman, M., & Yeh, J. K. (2006). Reference range for serum parathyroid hormone. *Endocrine Practice, 12*, 137–144.
8. Martin, T. J. (2004). Does bone resorption inhibition affect the anabolic response to parathyroid hormone? *Trends in Endocrinology and Metabolism, 15*, 49–50.
9. Chen, H., Heng, C. K., Puiu, P. D., Zhou, X. D., Lee, A. C., Lim, T. M., & Tan, S. N. (2005). Detection of *Saccharomyces cerevisiae* immobilized on self-assembled monolayer (SAM) of alkanethiolate using elec-trochemical impedance spectroscopy. *Analytica Chimica Acta, 554*, 52–59.
10. Wang, H. B., Zhang, H. D., Ping Xu, S., Gan, T., Huang, K. J., & Liu, Y. M. (2014). A sensitive and label-free electrochemical impedance biosensor for protein detection based on terminal protection of small molecule-linked DNA. *Sensors Actuators B Chem, 194*, 478–483.
11. Abdolahad, M., Shashaani, H., Janmaleki, M., & Mohajerzadeh, S. (2014). Silicon nanograss based impedance biosensor for label free detection of rare metastatic cells among primary cancerous colon cells, suitable for more accurate cancer staging. *Biosensors and Bioelectronics, 59*, 151–159.
12. Billah, M. M., Hodges, C. S., Hays, H. C. W., & Millner, P. A. (2010). Directed immobilization of reduced antibody fragments onto a novel SAM on gold for myoglobin impedance immunosensing. *Bioelectrochemistry, 80*, 49–54.
13. Asav, E., & Sezgintürk, M. K. (2014). A novel impedimetric disposable immunosensor for rapid detection of a potential cancer biomarker. *International Journal of Biological Macromolecules, 66*, 273–280.
14. Baldrich, E., Laczka, O., Del Campo, F. J., & Muñoz, F. X. (2008). Gold immuno-functionalisation via self-assembled monolayers: study of critical parameters and comparative performance for protein and bacteria detection. *Journal of Immunological Methods, 336*, 203–212.
15. van Wink, T., Zuilen, S. J., Bult, A., & van Bennekom, W. P. (1997). Self-assembled monolayers for biosensors. *Analyst, 122*, 43–50.
16. Vericat, C., Vela, M. E., & Salvarezza, R. C. (2005). Self-assembled monolayers of alkanethiols on Au (111): surface structures, defects and dynamics. *Physical Chemistry Chemical Physics, 7*, 3258–3268.

17. Hsieh, K. M., Lan, K. C., Hu, W. L., Chen, M. K., Jang, L. S., & Wang, M. H. (2013). Glycated hemoglobin ($HbA_{1c}$) affinity biosensors with ring-shaped interdigital electrodes on impedance measurement. *Biosensors and Bioelectronics, 49*, 450–456.
18. Sonuç, M. N., & Sezgintürk, M. K. (2014). Ultrasensitive electrochemical detection of cancer associated biomarker HER3 based on anti-HER3 biosensor. *Talanta, 120*, 355–361.
19. Sezgintürk, M. K., & Uygun, Z. O. (2012). An impedimetric vascular endothelial growth factor biosensor-based PAMAM/cysteamine-modified gold electrode for monitoring of tumor growth. *Analytical Biochemistry, 423*, 277–285.
20. Huang, I. Y., & Lee, M. C. (2008). Development of a FPW allergy biosensor for human IgE detection by MEMS and cystamine-based SAM technologies. *Sensors and Actuators B: Chemical, 132*, 340–348.
21. Hiasa, T., & Onishi, H. (2014). Mercaptohexanol assembled on gold: FM-AFM imaging in water. *Colloids and Surfaces A: Physicochemical and Engineering Aspects, 441*, 149–154.
22. Dittmer, W. U., Kievit, P., Prins, M. W. J., Vissers, J. L. M., Mersch, M. E. C., & Martens, M. F. W. C. (2008). Sensitive and rapid immunoassay for parathyroid hormone using magnetic particle labels and magnetic actuation. *Journal of Immunological Methods, 338*, 40–46.
23. Özcan, B., Demirbakan, B., Yeşiller, G., & Sezgintürk, M. K. (2014). Introducing a new method for evaluation of the interaction between an antigen and an antibody: single frequency impedance analysis for biosensing systems. *Talanta, 125*(2014), 7–13.